scientific reports

Check for updates

OPEN

The differential effect of Interferon-gamma on acute kidney injury and parasitemia in experimental malaria

Rebecca Sadler[1,5], Hendrik Possemiers[1,5], Fran Prenen[1], Lotte Van Landschoot[1], Emilie Pollenus[1], Margot Deckers[1,2], Sofie Knoops[1], Priyanka Koshy[3], Patrick Matthys[4] & Philippe E. Van den Steen[1]✉

Malaria-associated acute kidney injury (MAKI) is a common complication of *Plasmodium* infection, affecting ~ 50% of severe malaria cases and associated with increased mortality. However, its immunopathogenesis remains unclear. Interferon-gamma (IFN-gamma) is a crucial cytokine that influences parasite clearance and mediates pathogenesis in experimental models of malaria. This study explored the role of IFN-gamma in kidney pathology in C57BL/6 mice infected with *Plasmodium berghei* NK65 (*Pb*NK65) and *P. chabaudi* AS (*Pc*AS). *Pb*NK65-infected mice, normally susceptible to severe malaria, were protected from both MAKI and malaria-associated acute respiratory distress syndrome (MA-ARDS) when lacking IFN-gamma. Infected IFN-gamma knockout (KO) mice developed low parasitemia levels, minimal kidney histopathological changes and reduced expression of the kidney injury marker Neutrophil Gelatinase-Associated Lipocalin (NGAL). In contrast, upon *Pc*AS-infection, IFN-gamma deficiency led to increased parasitemia and aggravated kidney pathology, evidenced by proteinuria, hyaline casts in kidneys and increased renal mRNA expression of Heme Oxygenase 1 (HO-1) and NGAL. In both models, IFN-gamma induced renal C-X-C Motif Chemokine Ligand 10 (CXCL10) but did not affect Tumor Necrosis Factor-alpha (TNF-alpha) expression. Our data indicate that IFN-gamma exerts a dual effect on kidney pathology, which is conditioned by the mouse model and its impact on parasitemia.

Keywords Malaria, IFN-γ, Acute kidney injury, Inflammation

Malaria is caused by *Plasmodium* parasites and is one of the most important global infectious diseases. It accounts for over 249 million clinical cases and 600 000 deaths annually[1]. It primarily impacts tropical and subtropical regions, particularly sub-Saharan Africa. Young children and pregnant women are the most vulnerable populations in these regions. Malaria presents with a wide spectrum of clinical symptoms, ranging from a mild, flu-like illness to severe complications, including cerebral malaria (CM), severe malarial anemia, and malaria-associated acute respiratory distress syndrome (MA-ARDS)[2,3]. Over the past decade, the focus on malaria-associated acute kidney injury (MAKI) has steadily increased. Malaria is the primary cause of acute kidney injury (AKI) in sub-Saharan Africa, accounting for 50% of all AKI cases in the Democratic Republic of Congo[4,5]. MAKI is characterized by a sudden and rapid decline in renal function, resulting in an impaired ability of the kidney to effectively filter metabolic waste products, electrolytes, and excess fluids from the bloodstream[6]. MAKI has been associated with increased in-hospital mortality, post-discharge mortality, and neurologic deficits such as uremic encephalopathy[5].

Traditionally, three main hypotheses have been proposed that could explain the development of MAKI: intravascular hemolysis, insufficient blood flow due to parasite sequestration and an exaggerated host response[7]. Recent studies have already demonstrated the detrimental role of heme in the development of

[1]Laboratory of Immunoparasitology, Department of Microbiology, Immunology and Transplantation, Rega Institute of Medical Research, KU Leuven, Leuven, Belgium. [2]Laboratory of Host-Pathogen Interactions, Department of Pathology, University of Utah, Salt Lake City, United States of America. [3]Department of Pathology, University Hospitals Leuven, Leuven, Belgium. [4]Laboratory of Immunobiology, Department of Microbiology, Immunology and Transplantation, Rega Institute of Medical Research, KU Leuven, Leuven, Belgium. [5]Rebecca Sadler and Hendrik Possemiers contributed equally. ✉email: philippe.vandensteen@kuleuven.be

MAKI[8–10]. Previously, we have shown that kidney pathology in the *Plasmodium berghei* NK65 (*Pb*NK65) model is independent of parasite sequestration[11]. Nevertheless, the role of the host immune response in the development of MAKI remains unclear. Severe malaria triggers excessive proinflammatory cytokine production, such as Tumor Necrosis Factor-alpha (TNF-α), Interleukin-1β (IL-1β) and IL-6, in plasma of humans as well as in murine kidney tissues[12,13]. Additionally, a recent study found a correlation between circulating immune complexes and hemoglobinuria in children in Uganda[5]. Despite these insights, the full immunopathology of MAKI remains poorly understood.

Pro- and anti-inflammatory cytokines are essential to maintain the balance between immunity and pathology during malaria. This has been investigated and reviewed in detail in several mouse models of malaria[3]. Typically, in non-lethal models with a transient parasitemia peak such as *P. chabaudi* AS (*Pc*AS) in C57BL/6 mice, proinflammatory cytokines such as IL-12 and Interferon-γ (IFN-γ) are required for antiparasitic immunity. In contrast, in models with lethal *P. berghei* ANKA or *Pb*NK65 infections, these cytokines mediate lethal immunopathologies such as experimental CM and MA-ARDS[14,15]. Anti-inflammatory cytokines, such as IL-10, counterbalance these effects and downregulate both antiparasitic immunity and immunopathologies. IFN-γ is crucial for the T helper-type 1 (Th1) immune response and is produced by both the innate and adaptive immune system[3]. NK (T) cells and γδ T cells are the early producers of IFN-γ during a malaria infection, and subsequently the production shifts to activated $CD4^+$ and $CD8^+$ T cells as main producers of large amounts of IFN-γ[3]. While IFN-γ plays an important role in antimalarial immunity, its dysregulation can lead to complications[14], such as CM and MA-ARDS[15,16]. Besides being an essential cytokine for the Th1 immune response during malaria, IFN-γ is crucial for the expression of chemokines and adhesion molecules and subsequent $CD8^+$ T cell infiltrations in brain and lungs during experimental CM and MA-ARDS[16–18]. Furthermore, IFN-γ is essential for cross-presentation of malarial antigens by endothelial cells in these models[15,19]. In contrast, Th2 immune responses are typically less prominent in malaria[20].

Clinical studies have described both protective and pathological associations regarding the role of IFN-γ in malaria[14,21]. Elevated levels of proinflammatory cytokines, including IFN-γ, have been linked to the severity of CM and anemia in Malawian children[22]. A recent meta-analysis has found a correlation between IFN-γ levels and malaria severity[23]. Furthermore, IFN-γ is implicated in the pathogenesis of kidney conditions like lupus nephritis[24]and renal ischemic injury[25]. By upregulating major histocompatibility complex (MHC) on renal cells, it enhances antigen presentation, potentially promoting autoimmunity[26]. Multiple studies have identified an increased renal expression of IFN-γ during malaria infection[27,28]. Despite these insights, the exact role of IFN-γ in conveying protection or exacerbating MAKI remains poorly understood.

In this study, we examined the effect of IFN-γ deficiency on kidney pathology in experimental models of severe and mild malaria using *Pb*NK65 and *Pc*AS, respectively. IFN-γ knockout (KO) mice infected with *Pb*NK65 presented a delayed parasitemia development which did not reach similar levels as the wild type (WT) mice. Furthermore, these mice were protected from kidney pathology. In contrast, IFN-γ KO mice infected with *PcAS* presented with hyperparasitemia and exacerbated kidney pathology. These findings demonstrate that IFN-γ deficiency has a parasite strain-dependent effect on parasitemia and kidney pathology in murine malaria models.

Results

*Pb*NK65-infected IFN-γ KO mice do not develop kidney pathology

Previously, we observed the development of MAKI in *Pb*NK65-infected C57BL/6 mice, as evidenced by proteinuria, increased blood urea nitrogen (BUN) levels, renal inflammation and histopathological changes[11]. To determine the role of IFN-γ in the pathogenesis of experimental MAKI, both IFN-γ KO and WT mice were infected with *Pb*NK65. We observed significantly decreased parasitemia levels in *Pb*NK65-infected IFN-γ KO mice compared to WT mice from day 8 post infection (p.i.) (Fig. 1a). *Pb*NK65-infected IFN-γ KO mice also showed a milder disease course compared to the infected WT mice, with significantly lower clinical scores (Fig. 1b) and no decrease in body weight (Fig. 1c). At 9 days p.i., mice were dissected and alveolar edema was determined. Upon infection, IFN-γ KO mice did not develop alveolar edema, while significantly increased alveolar edema was observed in the WT mice (Fig. 1d). Furthermore, we studied the effect of IFN-γ on the kidney pathology by determining proteinuria and BUN plasma levels (Fig. 1e, f). Upon infection, WT mice developed significantly increased proteinuria and plasma BUN levels. However, this was not observed in IFN-γ KO mice.

To examine the contribution of IFN-γ signaling on renal histopathological changes during infection, we performed Periodic Acid Schiff (PAS) staining on kidney sections of control and *Pb*NK65-infected WT and IFN-γ KO mice. Glomerulosclerosis was detected with collapse of some glomerular capillary tufts, in kidneys of *Pb*NK65-infected WT mice at day 9 p.i. (Fig. 2a). Up to 9% of the glomeruli were affected in the *Pb*NK65-infected IFN-γ WT mice, which was significantly higher compared to *Pb*NK65-infected IFN-γ KO mice (Fig. 2b). Acute tubular injury, characterized by vacuolization of tubular epithelial cells and loss of brush border in proximal tubular epithelial cells, was present in infected WT mice, but not in IFN-γ KO mice (Fig. 2a). Intravascular accumulation of leukocytes was also observed in the kidneys of *Pb*NK65-infected WT mice, but not in IFN-γ KO mice.

To determine whether kidney pathology in IFN-γ KO mice developed later during infection, mice were followed up until 16 days p.i. **(Suppl. Fig S1).** Parasitemia in IFN-γ KO mice slowly increased, but did not reach similar levels as in IFN-γ WT mice. At 16 days p.i. mild proteinuria was observed in IFN-γ KO mice in the absence of alveolar edema or body weight loss. A positive correlation between parasitemia and proteinuria was observed. PAS staining of kidney sections showed only minimal histopathological alterations at day 16 p.i., in IFN-γ KO mice, with no collapsing glomeruli. However, mild tubular injury such as interstitial edema was

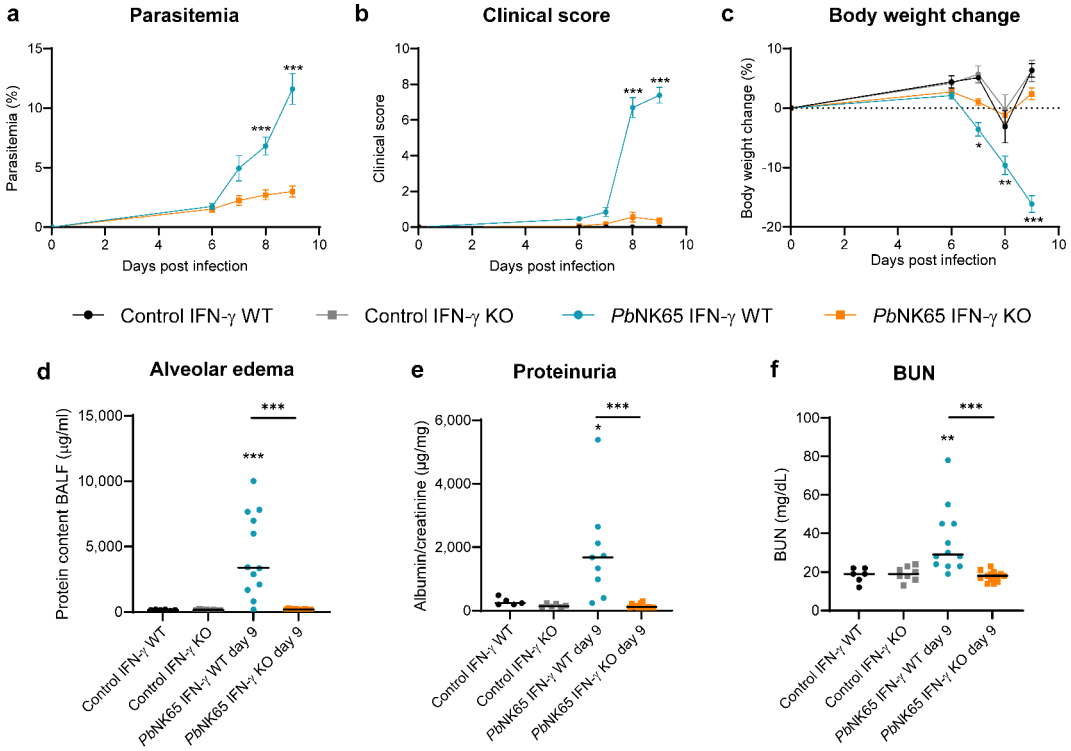

Fig. 1. ***Pb*NK65-infected IFN-γ KO mice develop decreased parasitemia levels without kidney pathology.** WT and IFN-γ KO C57BL/6 mice were infected with *Pb*NK65. (**a**) Peripheral parasitemia was determined on blood smears. (**b**) The clinical score and (**c**) body weight was monitored daily from 6 days p.i. onwards. Infected mice were euthanized and dissected at 9 days p.i. and (**d**) protein content in the broncho alveolar lavage fluid (BALF) was determined as measure for alveolar edema. (**e**) Albumin/creatinine ratios were determined in urine samples. (**f**) BUN values were determined in blood collected via retro-orbital puncture. Asterisks above data points indicate significant differences compared to control mice, asterisks above a horizontal line show significant differences between infected groups, $^{*}p < 0.05$, $^{**}p < 0.01$, $^{***}p < 0.001$. Data of two experiments, Control IFN-γ WT: $n = 6$, Control IFN-γ KO: $n = 8$, *Pb*NK65-infected IFN-γ WT mice: $n = 12$, *Pb*NK65-infected IFN-γ KO mice: $n = 14$. In panels **a-c**, data are represented as means +/- SEM. Mann-Whitney U test with Holm-Bonferroni correction for multiple testing was performed (number of tests = 4 in panels **c-f**).

observed in some mice (**Suppl. Fig S2**). In conclusion, our findings highlight the pathogenic role of IFN-γ in the *Pb*NK65 model, as its presence boosts parasitemia, and thereby exacerbates MAKI and MA-ARDS.

*Pc*AS-infected IFN-γ KO mice develop hyperparasitemia and increased proteinuria

To examine the effect of IFN-γ on kidney pathology in the *Pc*AS mouse model of mild malaria, we infected IFN-γ KO and WT mice with *Pc*AS parasites. *Pc*AS-infected IFN-γ KO mice developed significantly increased parasitemia levels compared to WT mice, with parasitemia levels up to 60% at day 9 and 10 p.i. (Fig. 3a). Furthermore, clinical scores were significantly higher in *Pc*AS-infected IFN-γ KO mice compared to *Pc*AS-infected WT mice (Fig. 3b). Body weight loss appeared more pronounced in IFN-γ KO mice, but this difference was only statistically different on day 9 p.i. (Fig. 3c). A subgroup of *Pc*AS-infected IFN-γ KO mice developed proteinuria at peak parasitemia (day 9 or 10 p.i.) with significantly increased proteinuria at day 9 p.i. compared to control mice (Fig. 3d). Furthermore, these mice also produced dark urine at peak parasitemia.

Interestingly, a clear gender difference was noted amongst the infected IFN-γ KO mice. Male IFN-γ KO mice developed higher parasitemia and increased proteinuria compared to female IFN-γ KO mice. In male mice, proteinuria and body weight loss were also significantly increased in the IFN-γ KO group compared to WT. This difference was not observed in the female mice (Fig. 3e and **Suppl. Fig. S3**). Increased parasitemia levels were positively correlated with proteinuria (Fig. 3f). Furthermore, no alveolar edema was observed, indicating the absence of MA-ARDS in both infected groups. (Suppl. **Fig. S4**).

*Pc*AS-infected IFN-γ KO mice develop mild tubular injury and hyaline casts in kidneys

To study the renal histopathology in *Pc*AS-infected IFN-γ KO and WT mice, PAS staining was performed on kidney sections (Fig. 4). Mild tubular injury, loss of the brush border, sloughing of epithelial cells and vacuolization were detected mainly in the cortex of kidneys of *Pc*AS-infected IFN-γ KO mice. This was not observed in the *Pc*AS-infected WT mice. No interstitial nephritis or interstitial edema was observed. The glomerular capillaries were open in both the *Pc*AS-infected WT and IFN-γ KO mice, indicating the absence of glomerular collapse.

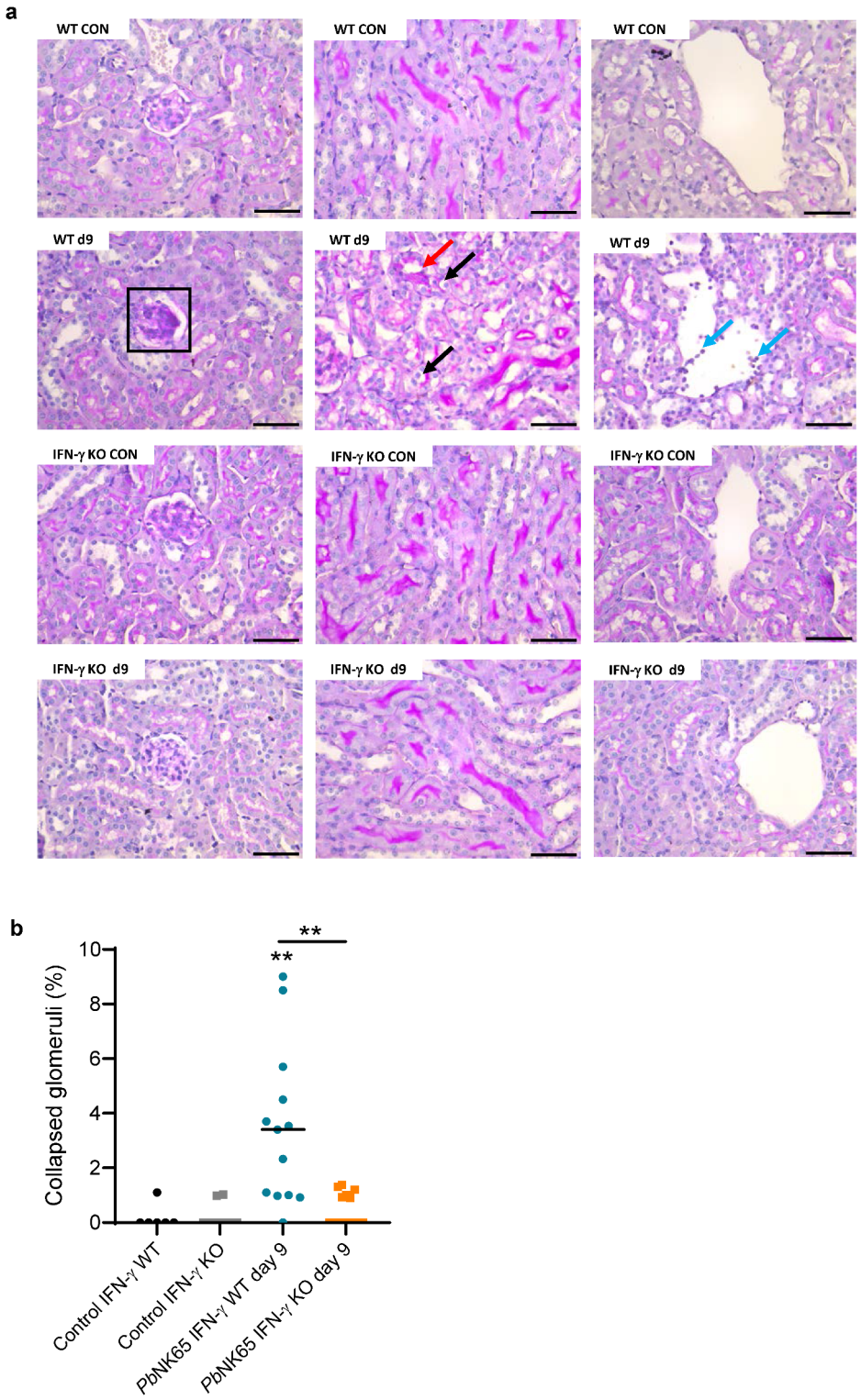

Fig. 2. Less glomerular collapse in *Pb*NK65-infected IFN-γ KO compared to WT mice. (**a**) Kidney sections were stained with PAS. Representative images are shown (original magnification x40, bar = 50 µm). Black frames indicate collapse of glomerular tufts. Black arrows indicate vacuolization of proximal tubular epithelial cells, red arrows indicate loss of brush border of proximal tubular epithelial cells. Blue arrows indicate vascular leukocyte accumulations. (**b**) Percentage of glomeruli with collapsed glomerular tufts counted on PAS-stained kidney sections. Asterisks above data points indicate significant differences compared to control mice, $^{**}p < 0.01$. Data of two experiments, Control IFN-γ WT: $n = 6$, Control IFN-γ KO: $n = 8$, *Pb*NK65-infected IFN-γ WT d9: $n = 13$, *Pb*NK65-infected IFN-γ KO d9: $n = 15$. Mann-Whitney U test with Holm-Bonferroni correction for multiple testing (number of tests = 4) was performed in panel **b**.

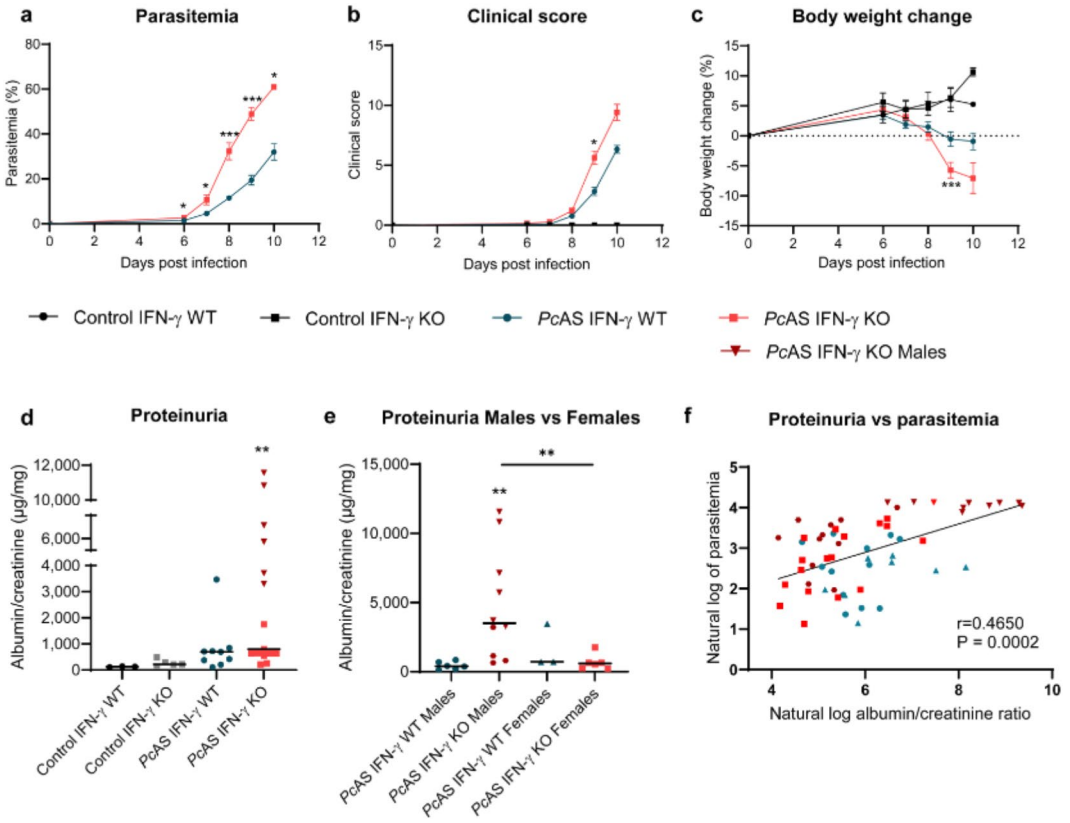

Fig. 3. ***Pc*AS-infected IFN-γ KO mice develop hyperparasitemia and increased kidney pathology.** IFN-γ KO and WT C57BL/6 mice were infected with *Pc*AS. (**a**) Peripheral parasitemia was determined on blood smears. (**b**) The clinical score and (**c**) body weight was monitored daily from day 6 p.i. onwards. Infected mice were euthanized and dissected at peak parasitemia at day 9 or 10 p.i. and (**d**) albumin/creatinine ratios were determined in urine samples. Asterisks above data points indicate significant differences compared to control mice, asterisks above a horizontal line show significant differences between infected groups. (**e**) Albumin/creatinine ratios were subdivided according to gender. Asterisks above data points indicate significant differences compared to IFN-γ WT infected mice of corresponding gender, asterisks above a horizontal line show significant differences between gender, $*p < 0.05$, $**p < 0.01$, $***p < 0.001$. (**f**) Correlation analysis of parasitemia with albumin/creatinine ratios of urine of *Pc*AS-infected IFN-γ WT and IFN-γ KO at day 7, 8, 9 and 10 p.i. Dark brown upside down triangles indicate *Pc*AS-infected IFN-γ KO which produced dark urine. Spearman correlation test was performed, Spearman correlation coefficient r and p-values are shown. Data of two experiments, Control IFN-γ WT: $n = 4$, Control IFN-γ KO: $n = 8$, *Pc*AS-infected IFN-γ WT mice: $n = 13$, *Pc*AS-infected IFN-γ KO mice: $n = 19$. Mann-Whitney U test with Holm-Bonferroni correction for multiple testing (number of tests = 4) was performed in panels **c**-**e**.

In the kidney sections of most *Pc*AS-infected IFN-γ KO mice, casts were detected in the lumen of the tubules (Fig. 5a). To confirm the presence of casts, hematoxylin-eosin (H&E) staining was performed on kidney sections from control mice and *Pc*AS-infected mice, revealing hyaline casts primarily in the lumen of the distal tubules (Fig. 5b). Importantly, the number of hyaline casts in the *Pc*AS-infected IFN-γ KO mice was significantly increased compared to the WT mice, further corroborating the increased renal injury (Fig. 5c). Interestingly, the largest number of hyaline casts were observed in infected male IFN-γ KO mice, further corroborating the gender difference in kidney pathology (**Suppl. Fig S3.**). Overall, these results indicate protective effects of IFN-γ in the *Pc*AS model, as its presence inhibits parasitemia, and thereby diminishes kidney pathology.

Expression of kidney injury markers and cytokines increased during malaria infection

MAKI pathogenesis is associated with elevated kidney injury markers and increased renal cytokine expression[11]. Therefore, we measured the expression of kidney injury markers and cytokines in the kidneys of infected and non-infected mice by qRT-PCR. The mRNA expression of the following markers was determined: Neutrophil Gelatinase-Associated Lipocalin (NGAL, released by the renal tubular cells in response to injury), Heme Oxygenase 1 (HO-1, induced upon and protective against oxidative stress), C-X-C Motif Chemokine Ligand 10 (CXCL10, also designated as IP-10; pathogenic in other malaria-induced complications by attracting activated T cells) and TNF-α (key proinflammatory cytokine). Upon infection with *Pb*NK65, the mRNA expression of NGAL was increased in both WT and IFN-γ KO mice at day 9 and 16 p.i., with significant differences between WT mice at 9 days p.i. and IFN-γ KO mice at 9 and 16 days p.i. (Fig. 6a). This is consistent with the minimal

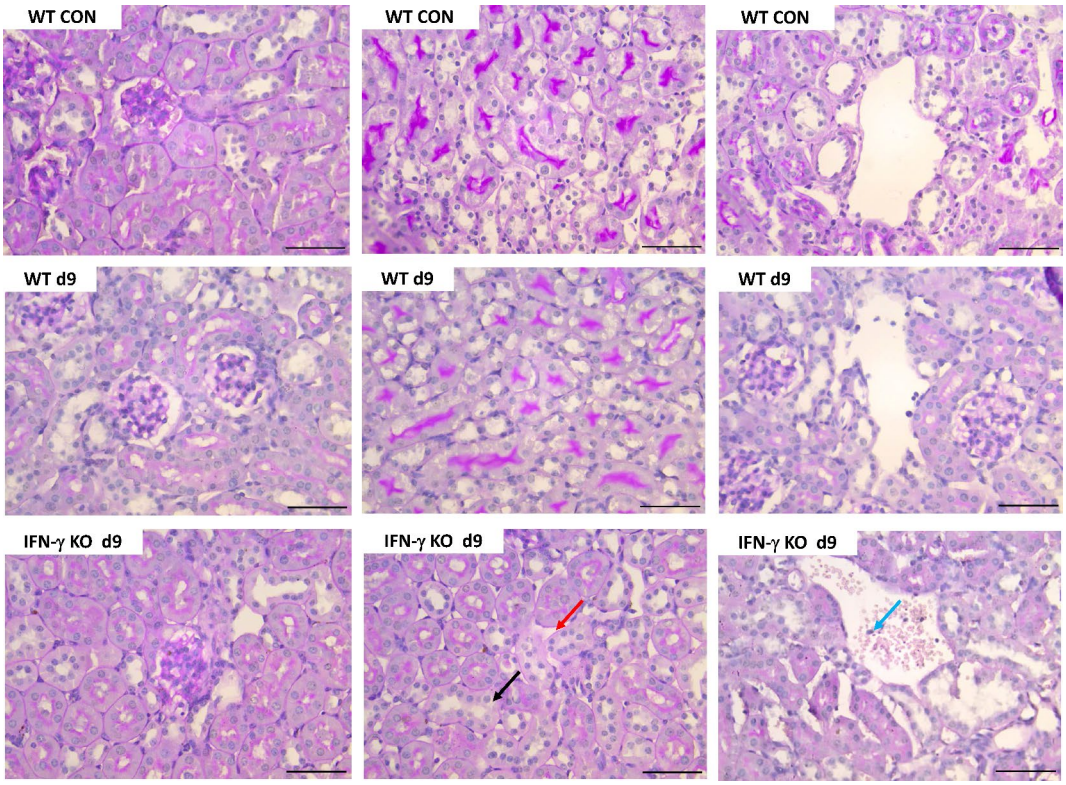

Fig. 4. ***Pc*AS-infection induces mild tubular injury in IFN-γ KO mice.** At day 9 or day 10 p.i. (peak parasitemia), control, WT and IFN-γ KO C57BL/6 mice infected with *Pc*AS were killed and dissected. PAS staining was performed (original magnification x40, bar = 50 µm). Black arrows indicate vacuolization of proximal tubular epithelial cells, red arrows indicate loss of brush border of proximal tubular epithelial cells. Blue arrows indicate vascular accumulation of leukocytes.

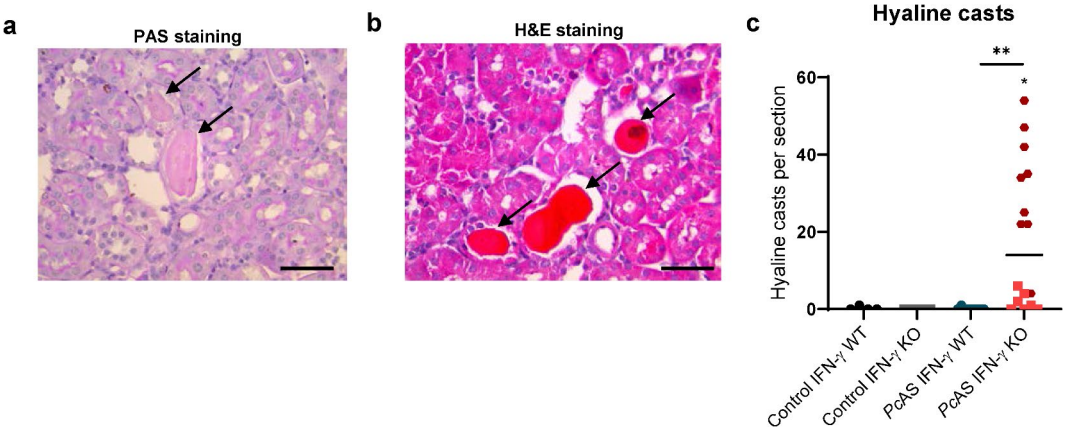

Fig. 5. **Hyaline casts are formed in *Pc*AS-infected IFN-γ KO mice.** At day 9 or day 10 p.i. (peak parasitemia) IFN-γ KO C57BL/6 mice infected with *Pc*AS were dissected. (**a**) PAS staining and (**b**) H&E staining were performed (original magnification x40, bar = 50 µm). Casts are indicated with a black arrow on both the PAS and H&E staining. (**c**) Casts on H&E stained sections were counted. The gender of the infected IFN-γ KO mice is indicated by dark red for males and bright red for females. Asterisks above data points indicate significant differences compared to control mice, asterisks above a horizontal line show significant differences between KO and WT infected groups, $^{*}p < 0.05$, $^{**}p < 0.01$, $^{***}p < 0.001$. Data of two experiments, Control IFN-γ WT: $n = 4$, Control IFN-γ KO: $n = 8$, *Pc*AS-infected IFN-γ WT mice: $n = 13$, *Pc*AS-infected IFN-γ KO mice: $n = 19$. Mann-Whitney U test with Holm-Bonferroni correction for multiple testing (number of tests = 4) was performed in panel **c**.

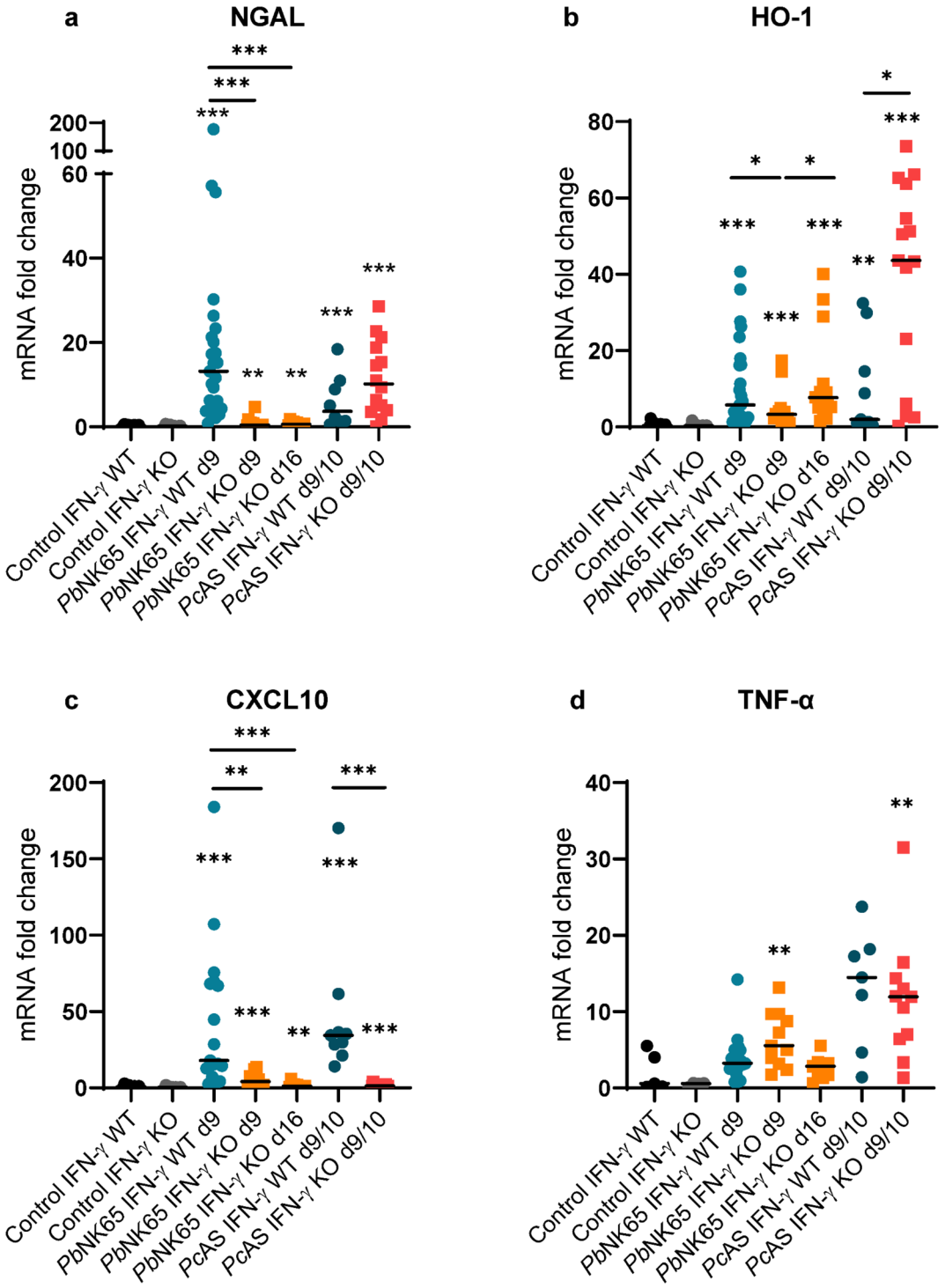

Fig. 6. Kidney injury markers and cytokines increased during malaria infection. IFN-γ KO and WT C57BL/6 mice were infected with *Pb*NK65 and *Pc*AS. The kidneys were collected at day 9 p.i. and day 16 p.i. for *Pb*NK65-infected mice and at day 9 or 10 p.i. (peak parasitemia) for *PcAS*-infected mice. RT-qPCR was performed on the kidneys. (**a**) mRNA expression of NGAL and (**b**) HO-1 were measured. (**c**) Inflammatory cytokines CXCL10 and (**d**) TNF-α were measured. Asterisks above data points indicate significant differences compared to control mice, asterisks above a horizontal line show significant differences between infected groups, $^{*}p < 0.05$, $^{**}p < 0.01$, $^{***}p < 0.001$. Mann-Whitney U test with Holm-Bonferroni correction for multiple testing (number of tests = 10 (no comparisons between parasite strains)) was performed in all panels.

kidney injury in the *Pb*NK65-infected IFN-γ KO mice. The mRNA of HO-1, which is typically induced by heme and protects against oxidative damage, was also increased in *Pb*NK65-infected mice. Moreover, HO-1 was significantly more increased in WT than in IFN-γ KO mice at 9 days p.i., though no difference was observed anymore between WT mice at 9 days p.i. and IFN-γ KO mice at 16 days p.i. In *Pc*AS-infected mice, both HO-1 and NGAL mRNA levels were increased compared to control mice, with only HO-1 being significantly higher in IFN-γ KO compared to WT (Fig. 6b). Both *Pb*NK65 and *Pc*AS infections led to increased renal CXCL10 mRNA expression, with significantly lower levels in IFN-γ KO mice compared to WT mice (Fig. 6c). TNF-α mRNA expression did not differ between WT and KO, but was significantly different from controls in KO-infected mice (Fig. 6d). These data confirm the presence of kidney pathology, and indicate that IFN-γ is important for the induction of CXCL10 in both models. Furthermore, the effect of IFN-γ on the expression of NGAL and HO-1 is dependent on the used parasite strain.

Materials and methods

Parasites and mice

Seven to eight weeks old WT and IFN-γ KO mice, 8 times backcrossed to C57BL/6 and obtained from Jackson Laboratories (strain #002287), were bred in the animal house of the Rega Institute for Medical Research, KU Leuven. All mice were housed in individually ventilated cages in a 12 h light and 12 h dark cycle in SPF animal facility. Drinking water was supplemented with 4-amino benzoic acid (0.422 mg/ml PABA, Sigma-Aldrich, Bornem, Belgium) and the mice had unlimited access to high energy food. IFN-γ WT and IFN-γ KO C57BL/6 mice were infected with *P. berghei* NK65 (*Pb*NK65) or *P. chabaudi* AS (*Pc*AS) parasites by intraperitoneal (IP) injection of 10^4iRBCs as described previously[29].

Scoring of disease progression and parasitemia determination

Starting from day 6 p.i., parasitemia, body weight and clinical score were evaluated daily starting from day 6 p.i. Blood smears of tail blood were stained with 10% Giemsa (VWR, Heverlee, Belgium) and parasitemia was calculated by microscopic analysis. Urine collection was performed daily. The clinical score was calculated by evaluating different clinical parameters, including social activity (SA), limb grasping (LG), body tone (BT), trunk curl (TC), pilo-erection (PE), shivering (Sh), abnormal breathing (AB), dehydration (D), incontinence (I) and paralysis (P). A score of 0 (absent) or 1 (present) was given for TC, PE, Sh and AB and 0 (normal), 1 (intermediate) or 2 (most serious) for the other parameters. The total clinical score was calculated using the following formula: SA + LG + BT + TC + PE + 3 * (Sh + AB + D + I + P). The mice were euthanized when the body weight decrease was > 20% compared to day 0 p.i. or when clinical score reached 10 or more[11,30].

Retro-orbital puncture and dissection

IFN-γ WT and IFN-γ KO mice infected with *Pb*NK65, dissected at day 9 p.i., were anesthetized with 3% isoflurane (Iso-Vet, Dechra, Nortwhich, United Kingdom) before retro-orbital puncture was performed with a heparinized (LEO Pharma, Lier, Belgium) glass capillary tube (Hirschmann-Laborgeräte, Eberstadt, Germany). The collected blood was analyzed with the Epoc Blood Analysis System (Siemens, Munich, Germany) to determine BUN levels. After the blood collection, mice were euthanized by performing heart puncture under anesthesia with 3% isoflurane.

The *Pc*AS-infected IFN-γ WT and IFN-γ KO mice were euthanized with Dolethal (Vétoquinol, Aartselaar, Belgium; 200 mg/mL, IP injection of 100 µL) followed by heart puncture at indicated time points. Broncho-alveolar lavage fluid (BALF) was collected by clamping off the left lung and catheterizing the bronchus of the mice. A total of 500 µl of PBS was infused through the catheter, then withdrawn after 30 s. This process was repeated, and the two samples were combined. The pooled BALF was then centrifuged at 314 g for 10 min at 4 °C, and the supernatant was collected. After a transcardial perfusion with 20 ml PBS, the left kidney was removed and laterally cut into two equal pieces and fixed in 4% formaldehyde for 48 h at 4 °C.

Kidney histology

After fixation for 48 h at 4 °C, kidney tissues were dehydrated by applying gradually increasing ethanol concentrations in the Excelsior MS tissue processor (Thermo Fisher Scientific, Waltham, USA). Next, the tissues were embedded in paraffin with the HistoStar Workstation (Thermo Fisher Scientific) and 5 µm thick tissue sections were made using a Microm HM 355 S microtome (Thermo Fisher Scientific). Tissue sections were stained with the Periodic Acid Schiff's (PAS) staining kit (Carl Roth GmbH, Karlsruhe, Germany) and Hematoxylin and eosin (H&E) staining (Abcam, Ab245880). Histological assessment was performed with a Leica DM 2000 microscope and pictures were taken using the LAS V4.2 Software (Leica). The percentage of collapsed glomeruli and renal blood vessels with intravascular accumulation of one or more leukocytes was calculated on whole sections. To quantify the casts, the kidney sections were blinded and the number of casts were counted per kidney section.

Analysis of urine samples

Urine samples were collected in a 1.5 mL Eppendorf tube at the indicated time points in the morning. The albumin/creatinine ratio in the urine was determined to assess proteinuria and kidney function as described in Vandermosten et al.[31].

Alveolar edema measurement

Alveolar edema formation was assessed by the quantification of the protein concentration in the supernatants of BALF using a Bradford assay (Bio-Rad).

Quantitative reverse transcription-polymerase chain reaction (qRT-PCR)

RNeasy Mini Kit (Qiagen, Hilden, Germany) was used to extract RNA from the kidney after mechanical homogenization in RLT buffer. After extraction, RNA was quantified and cDNA was synthesized using the High Capacity cDNA Reverse Transcription Kit (Applied Biosystems, Waltham, USA). ABI Prism 7500 Sequence Detection System (Applied Biosystems) was used to perform qRT-PCR reaction on cDNA with specific primers (IDT, Leuven, Belgium, Table 1) in the TaqMan® Fast Universal PCR master mix (Applied Biosystems). The relative mRNA expression was determined as $2^{-\Delta\Delta CT}$, normalized to the mean 2^{-CT} value of the uninfected control mice and to the 2^{-CT} value of the 18 S housekeeping gene.

Statistical analysis

Statistical analysis was done using the GraphPad Prism software (GraphPad software, San Diego, USA, version 8.3.1). The non-parametric Mann–Whitney U test was used to determine the statistical significance between two groups. P-values smaller than 0.05 were considered statistically significant. P-values were defined as follows: $^{*}p<0.05$, $^{**}p<0.01$, $^{***}p<0.001$, $^{****}p<0.0001$. To correct for multiple testing, the Holm-Bonferroni method was applied and the number of comparisons are indicated in the figure legends. Unless otherwise specified, each dot represents an individual mouse. Horizontal lines represent group medians. Asterisks without horizontal lines represent significant differences compared to the control group, unless mentioned otherwise. Horizontal lines with asterisk on top indicate significant differences between infected groups, unless mentioned otherwise. Correlation analyses on non-normally distributed data were performed using the Spearman correlation analysis and linear regression was used for curve fitting.

Discussion

In this study, we investigated the role of IFN-γ, a crucial proinflammatory cytokine, in kidney pathology in experimental models of severe and mild malaria with *Pb*NK65 and *Pc*AS, respectively. Our results suggest that the effect of IFN-γ on the parasitemia indirectly affects kidney pathology (Fig. 7). These findings indicate that IFN-γ has a pathogenic effect in the *Pb*NK65 model, since IFN-γ deficiency resulted in delayed parasitemia levels and milder kidney pathology. In contrast, IFN-γ has a protective effect in the *Pc*AS model, as IFN-γ deficient mice developed higher parasitemia and more pronounced kidney pathology.

Consistent with our *Pc*AS data, previous studies have shown that IFN-γ promotes parasite clearance in both liver and blood stages of malaria[14,32,33]. A meta-analysis in children confirmed the protective effect of IFN-γ against parasitemia and anemia[34,35]. In the *Pc*AS model, IFN-γ is protective due to its proinflammatory roles in activating macrophages, promoting Th1 differentiation, and enhancing antigen presentation[14]. Moreover, A/J mice, which are highly susceptible to *Pc*AS, expressed lower levels of IFN-γ compared to resistant C57BL/6 mice[36].

In the *Pb*NK65 model, we observed a stimulating effect of IFN-γ on parasitemia. This was surprising, since other studies with *P. berghei* models described no effect of IFN-γ deficiency on parasitemia[17]. Therefore, this phenotype might be specific for *Pb*NK65. However, IFN-γ has been shown to mediate increased total parasite burden of *P. berghei* ANKA[27], which may be explained by the induction of adhesion molecules that may mediate parasite sequestration[16,17]. Interestingly, Guthmiller et al. observed that IFN-γ signaling in B cells reduces the production of anti-plasmodial antibodies in a model with *P. yoelii*, suggesting that IFN-γ may also inhibit antimalarial immunity[37].

Previously, the pathological role of IFN-γ has been observed using a monoclonal antibody against IFN-γ in a CM model[38]. Lung and brain pathology in the *Pb*NK65 and *Pb*ANKA models are driven by $CD8^+$ T cells, which has been demonstrated in multiple studies[15–17,30]. Notably, upon severe malaria infection, $CD8^+$ T cells express high levels of IFN-γ[15]. The $CD8^+$ T cell-driven pathology requires IFN-γ-induced cross-presentation of malarial antigens by endothelial cells. Furthermore, the IFN-γ-dependent induction of chemokines and adhesion molecules is also critical for the pathology[15,16,39]. In contrast, the *Pc*AS model is less dependent on $CD8^+$ T cell-mediated pathology[40]. Our study offers novel insight into the role of IFN-γ on parasitemia with an indirect immunopathological effect on MAKI. The immunopathogenesis in MAKI has been poorly investigated, although 50% of severe malaria patients present with MAKI[5]. Overall, we report improved *versus* exacerbated kidney pathology in the *Pb*NK65 and *Pc*AS model of malaria with deficiency of IFN-γ, respectively. Exacerbated kidney pathology was also marked by increased proteinuria, and an increase in mRNA expression of HO-1 in the *Pc*AS model and NGAL in the *Pb*NK65 model.

Our data suggest that parasitemia is strongly associated with kidney pathology in malaria. This may correspond with the known role of intravascular hemolysis in MAKI[10,41,42]. In particular, increased hyaline cast depositions were also observed in haptoglobin/hemopexin double KO mice and in mice with kidney-specific deletion of

Predesigned qPCR assays (IDT)		
Name	Exon location	Assay ID
RNA18S	Exon 1–1	Hs.PT.39a.22214855
CXCL10	Exon 1–2	Mm.PT.58.43575827
HO-1	Exon 3–4	Mm.PT.58.8600055
NGAL	Exon 2–4	Mm.PT.58.10167155
TNF-α	Exon 2–4	Mm.PT.58.12575861

Table 1. List of primers used for RT-qPCR.

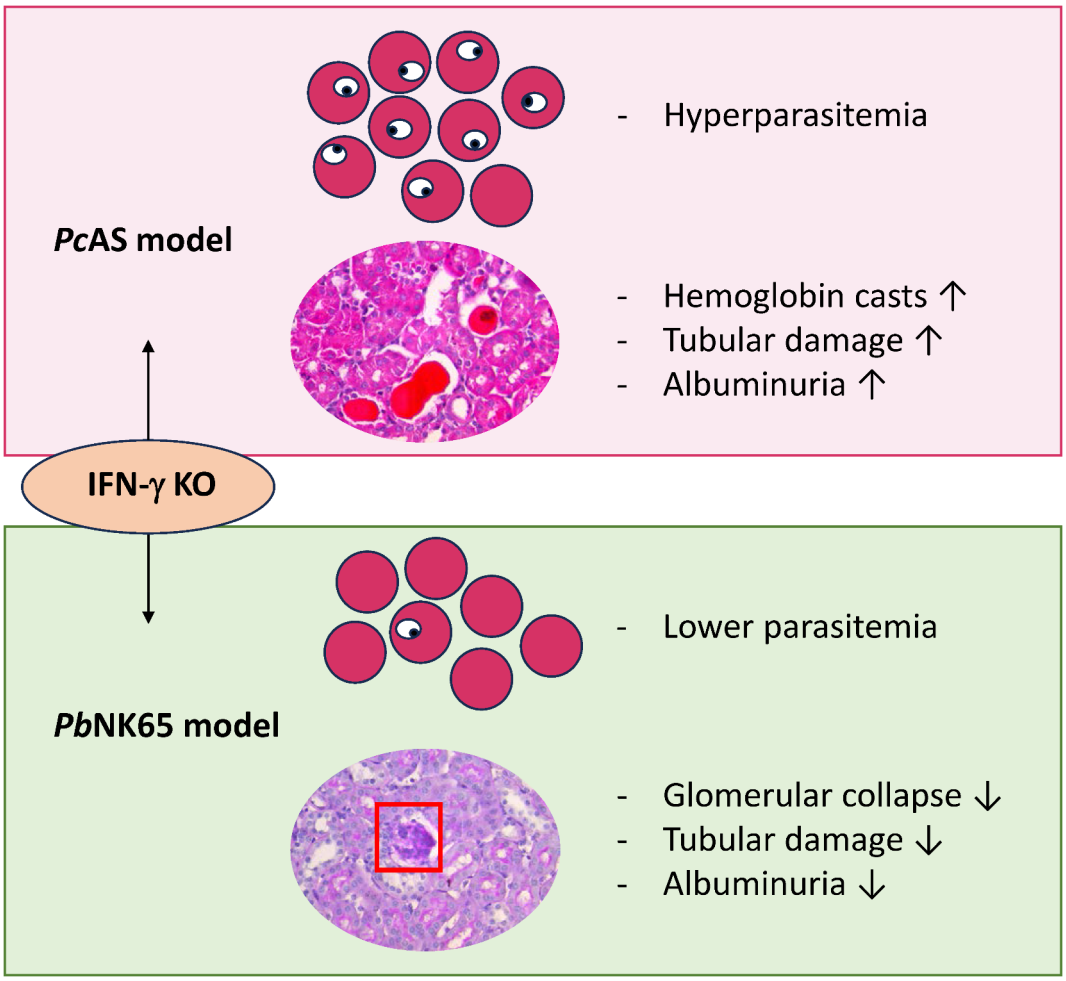

Fig. 7. Graphical abstract. The effect of IFN-γ KO differs in the *Pc*AS-infected versus *Pb*NK65-infected mice. In *Pc*AS-infected mice, IFN-γ deficiency result in hyperparasitemia, hemoglobin casts deposition, increased tubular damage and albuminuria. In contrast, IFN-γ deficiency in *Pb*NK65-infected mice results in low parasitemia, reduced glomerular collapse, tubular damage and albuminuria.

HO-1 or Ferritin-H upon *P. chabaudi* infection[10,43]. This suggests that the increased hemolysis associated with high parasitemia levels may overwhelm the haptoglobin / hemopexin / HO-1 / ferritin protective mechanisms, resulting in damage to the proximal epithelial tubules. The parasitemia in the *Pb*NK65 model is lower than in the *Pc*AS model. While we cannot exclude a role for a possibly higher load of sequestered *Pb*NK65 parasites, the presence of glomerular collapse suggests a different pathogenesis, which is currently insufficiently understood. The absence of glomerular collapse in *Pb*NK65-infected IFN-γ KO mice suggests either a direct role of IFN-γ, or a minimal parasitemia required to cause this glomerular pathology. Additionally, hemozoin is a known inducer of HO-1, CXCL10 and TNF-α in the liver and lungs[44,45]. Although the levels of hemozoin in the kidney is lower than in the liver and lungs[46], hemozoin might also contribute to the glomerular and tubular damage.

Multiple studies in humans have investigated the cytokine pattern during malaria infections. Although, the majority report IFN-γ to have protective effects, many also report the opposite. A study performed in Sri Lanka described an inverse relationship between IFN-γ and parasitemia, suggesting an anti-parasitic effect[34]. On the other hand, IFN-γ profiles where higher in Malawian and Indian children with severe malaria compared to uncomplicated malaria[22,47]. In another study, adults also presented with increased levels of IFN-γ correlating with severe malaria[48]. Interestingly, a recent meta-analysis reported a positive association between IFN-γ levels and malaria severity. However, the degree of heterogeneity among included studies was high[23]. This suggests that the role IFN-γ plays during malaria remains bivalent and needs further investigation.

Overall, our study provides new insights in the complex role of IFN-γ in the development of kidney injury in relation to parasitemia levels. Our data demonstrate that the effect of IFN-γ on kidney pathology is dependent on the model, and is mostly related to its effects on parasitemia. Further investigations are required to delineate the precise contribution of local inflammation and immunopathology to the pathogenesis of MAKI.

Data availability

All relevant data supporting the findings of this study are available within the article or its supporting information.

Received: 4 November 2024; Accepted: 13 February 2025
Published online: 21 February 2025

References

1. World Health Organization. Malaria. (2023). https://www.who.int/news-room/fact-sheets/detail/malaria
2. Moxon, C. A., Gibbins, M. P., Mcguinness, D., Milner, D. A. & Marti, M. New insights into malaria pathogenesis. *Annu. Rev. Pathol.* **15**, 315–343 (2019).
3. Deroost, K., Pham, T. T. & Opdenakker, G. Van Den Steen, P. E. The immunological balance between host and parasite in malaria. *FEMS Microbiol. Rev.* **40**, 208–257 (2016).
4. Nkoy, A. B. et al. A promising pediatric peritoneal dialysis experience in a resource-limited setting with the support of saving young lives program. *Perit. Dial Int.* **40**, 504–508 (2020).
5. Namazzi, R. et al. Acute kidney injury, persistent kidney disease, and post-discharge morbidity and mortality in severe malaria in children: a prospective cohort study. *EClinicalMedicine.* **44**, 101292 (2022).
6. Basile, D. P., Anderson, M. D. & Sutton, T. A. Pathophysiology of acute kidney injury. in *Compr Physiol* vol. 2 1303–1353 (2012).
7. Katsoulis, O., Georgiadou, A. & Cunnington, A. J. Immunopathology of acute kidney injury in severe malaria. *Front. Immunol.* **12**, 651739 (2021).
8. Gozzelino, R. et al. Metabolic adaptation to tissue iron overload confers tolerance to malaria. *Cell. Host Microbe.* **12**, 693–704 (2012).
9. Zarjou, A. et al. Proximal tubule H-ferritin mediates iron trafficking in acute kidney injury. *J. Clin. Invest.* **123**, 4423–4434 (2013).
10. Ramos, S. et al. Targeting circulating labile heme as a defense strategy against malaria. *Life Sci. Alliance.* **7**, e202302276 (2024).
11. Possemiers, H. et al. Experimental malaria-associated acute kidney injury is independent of parasite sequestration and resolves upon antimalarial treatment. *Front. Cell. Infect. Microbiol.* **12**, 915792 (2022).
12. Lyke, K. E. et al. Serum levels of the proinflammatory cytokines Interleukin-1 Beta (IL-1β), IL-6, IL-8, IL-10, Tumor necrosis factor alpha, and IL-12(p70) in Malian children with severe *Plasmodium Falciparum* malaria and matched uncomplicated malaria or healthy controls. *Infect. Immun.* **72**, 5630–5637 (2004).
13. Sinniah, R., Rui-Mei, L. & Kara, A. Up-regulation of cytokines in glomerulonephritis associated with murine malaria infection. *Int. J. Exp. Pathol.* **80**, 87–95 (1999).
14. King, T. & Lamb, T. Interferon-γ: the Jekyll and Hyde of malaria. *PLoS Pathog.* **11**, e1005118 (2015).
15. Claser, C. et al. Lung endothelial cell antigen cross-presentation to CD8 + T cells drives malaria-associated lung injury. *Nat. Commun.* **10**, 4241 (2019).
16. Van den Steen, P. E. et al. CXCR3 determines strain susceptibility to murine cerebral malaria by mediating T lymphocyte migration toward IFN-γ-induced chemokines. *Eur. J. Immunol.* **38**, 1082–1095 (2008).
17. BELNOUE, E. et al. Control of pathogenic CD8 $^{+}$ T cell migration to the brain by IFN-γ during experimental cerebral malaria. *Parasite Immunol.* **30**, 544–553 (2008).
18. Galvão-Filho, B. et al. The emergence of pathogenic TNF/iNOS producing dendritic cells (Tip-DCs) in a malaria model of acute respiratory distress syndrome (ARDS) is dependent on CCR4. *Mucosal Immunol.* **12**, 312–322 (2019).
19. Howland, S. W., Claser, C., Poh, C. M., Gun, S. Y. & Rénia, L. Pathogenic CD8 + T cells in experimental cerebral malaria. *Semin Immunopathol.* **37**, 221–231 (2015).
20. Perez-Mazliah, D. & Langhorne, J. CD4 T-Cell subsets in malaria: TH1/TH2 revisited. *Front. Immunol.* **5**, 671 (2015).
21. McCall, M. B. B. & Sauerwein, R. W. Interferon-γ—central mediator of protective immune responses against the pre-erythrocytic and blood stage of malaria. *J. Leukoc. Biol.* **88**, 1131–1143 (2010).
22. Mandala, W. L. et al. Cytokine profiles in Malawian children presenting with uncomplicated malaria, severe malarial anemia, and cerebral malaria. *Clin. Vaccine Immunol.* **24**, e0053316 (2017).
23. Mahittikorn, A. et al. Author correction: increased interferon-γ levels and risk of severe malaria: a meta-analysis. *Sci. Rep.* **12**, 21370 (2022).
24. Harigai, M. et al. Excessive production of IFN-γ in patients with systemic lupus erythematosus and its contribution to induction of B lymphocyte stimulator/B cell-activating factor/TNF ligand superfamily-13B. *J. Immunol.* **181**, 2211–2219 (2008).
25. Burne, M. J. et al. Identification of the CD4 + T cell as a major pathogenic factor in ischemic acute renal failure. *J. Clin. Invest.* **108**, 1283–1290 (2001).
26. Cheah, P. L., Looi, L. M., Chua, C. T., Yap, S. F. & Fleming, S. Enhanced major histocompatibility complex (MHC) class II antigen expression in lupus nephritis. *Malays J. Pathol.* **19**, 115–120 (1997).
27. Amante, F. H. et al. Immune-mediated mechanisms of parasite tissue sequestration during experimental cerebral malaria. *J. Immunol.* **185**, 3632–3642 (2010).
28. Tan, R. S. P., Feng, C., Asano, Y. & Kara, A. U. Altered immune response of Interferon regulatory factor 1-deficient mice against *Plasmodium berghei* blood-stage malaria infection. *Infect. Immun.* **67**, 2277–2283 (1999).
29. Van den Steen, P. E. et al. Immunopathology and dexamethasone therapy in a new model for malaria-associated acute respiratory distress syndrome. *Am. J. Respir Crit. Care Med.* **181**, 957–968 (2010).
30. Pollenus, E. et al. Single cell RNA sequencing reveals endothelial cell killing and resolution pathways in experimental malaria-associated acute respiratory distress syndrome. *PLoS Pathog.* **20**, e1011929 (2024).
31. Vandermosten, L. et al. Adrenal hormones mediate disease tolerance in malaria. *Nat. Commun.* **9**, (2018).
32. Cabantous, S. et al. Evidence that Interferon-γ plays a protective role during cerebral malaria. *J. Infect. Dis.* **192**, 854–860 (2005).
33. Drewry, L. L., Pewe, L. L., Hancox, L. S., Van de Wall, S. & Harty, J. T. CD4 T cell–dependent and –independent roles for IFN-γ in blood-stage malaria. *J. Immunol.* **210**, 1305–1313 (2023).
34. Perera, M. K. et al. Association of high plasma TNF-alpha levels and TNF-alpha/IL-10 ratios with TNF2 allele in severe *P. falciparum* malaria patients in Sri Lanka. *Pathog Glob Health.* **107**, 21–29 (2013).
35. Oyegue-Liabagui, S. L. et al. Pro- and anti-inflammatory cytokines in children with malaria in Franceville, Gabon. *Am. J. Clin. Exp. Immunol.* **6**, 9–20 (2017).
36. Jacobs, P., Radzioch, D. & Stevenson, M. M. A Th1-associated increase in tumor necrosis factor alpha expression in the spleen correlates with resistance to blood-stage malaria in mice. *Infect. Immun.* **64**, 535–541 (1996).
37. Guthmiller, J. J., Graham, A. C., Zander, R. A., Pope, R. L. & Butler, N. S. Cutting edge: IL-10 is essential for the generation of germinal center B cell responses and anti- *Plasmodium* humoral immunity. *J. Immunol.* **198**, 617–622 (2017).
38. Grau, G. E. et al. Monoclonal antibody against interferon gamma can prevent experimental cerebral malaria and its associated overproduction of tumor necrosis factor. *Proc. Natl. Acad. Sci.* **86**, 5572–5574 (1989).
39. Campanella, G. S. V. et al. Chemokine receptor CXCR3 and its ligands CXCL9 and CXCL10 are required for the development of murine cerebral malaria. *Proc. Natl. Acad. Sci.* **105**, 4814–4819 (2008).
40. Horne-Debets, J. M. et al. PD-1 dependent exhaustion of CD8 + T cells drives chronic Malaria. *Cell. Rep.* **5**, 1204–1213 (2013).

41. Plewes, K. et al. Cell-free hemoglobin mediated oxidative stress is associated with acute kidney injury and renal replacement therapy in severe falciparum malaria: an observational study. *BMC Infect. Dis.* **17**, 313 (2017).
42. Barber, B. E. et al. Intravascular haemolysis in severe *Plasmodium knowlesi* malaria: association with endothelial activation, microvascular dysfunction, and acute kidney injury. *Emerg. Microbes Infect.* **7**, 1–10 (2018).
43. Ramos, S. et al. Renal control of disease tolerance to malaria. *Proc. Natl. Acad. Sci.* **116**, 5681–5686 (2019).
44. Deroost, K. et al. Hemozoin induces lung inflammation and correlates with malaria-associated acute respiratory distress syndrome. *Am. J. Respir Cell. Mol. Biol.* **48**, 589–600 (2013).
45. Deroost, K. et al. Hemozoin induces hepatic inflammation in mice and is differentially associated with liver pathology depending on the Plasmodium strain. *PLoS One*. **9**, e113519 (2014).
46. Deroost, K. et al. Improved methods for haemozoin quantification in tissues yield organ-and parasite-specific information in malaria-infected mice. *Malar. J.* **11**, 166 (2012).
47. Prakash, D. et al. Clusters of cytokines determine malaria severity in *Plasmodium falciparum*– infected patients from endemic areas of central India. *J. Infect. Dis.* **194**, 198–207 (2006).
48. Wroczyńska, A., Nahorski, W., Bąkowska, A. & Pietkiewicz, H. Cytokines and clinical manifestations of malaria in adults with severe and uncomplicated disease. *Int. Marit Health*. **56**, 103–114 (2005).

Author contributions
PVdS and HP conceived the study. HP, LVL, FP, RS, EP, MD, SK performed the experiments. HP, RS, LVL, PK analyzed the data. RS and HP wrote the drafts of the manuscript. PM provided critical advice and essential materials. All authors critically read and edited the manuscript. All authors read and approved the final manuscript.

Funding
This study was supported by grants from the Research Foundation Flanders (F.W.O.-Vlaanderen, project G0C9720N and G066723N) and the Research Fund of KU Leuven (project C14/23/143). Dr. Hendrik Possemiers is a recipient of a F.W.O.-Vlaanderen PhD fellowship and Dr. Emilie Pollenus is a recipient of the L'Oréal-Unesco Women for Sciences and F.W.O.-Vlaanderen PhD fellowship.

Declarations

Competing interests
The authors declare no competing interests.

Ethical statement
All experiments at the KU Leuven were performed according to the regulations of the European Union (directive 2010/63/EU) and the Belgian Royal Decree of 29 May 2013, and were approved by the Animal Ethics Committee of the KU Leuven (License LA1210186, project P123/2022, Belgium). The study is reported in accordance with ARRIVE guidelines (https://arriveguidelines.org).

Additional information
Supplementary Information The online version contains supplementary material available at https://doi.org/10.1038/s41598-025-90473-7.

Correspondence and requests for materials should be addressed to P.E.V.d.S.

Reprints and permissions information is available at www.nature.com/reprints.

Publisher's note Springer Nature remains neutral with regard to jurisdictional claims in published maps and institutional affiliations.

Open Access This article is licensed under a Creative Commons Attribution-NonCommercial-NoDerivatives 4.0 International License, which permits any non-commercial use, sharing, distribution and reproduction in any medium or format, as long as you give appropriate credit to the original author(s) and the source, provide a link to the Creative Commons licence, and indicate if you modified the licensed material. You do not have permission under this licence to share adapted material derived from this article or parts of it. The images or other third party material in this article are included in the article's Creative Commons licence, unless indicated otherwise in a credit line to the material. If material is not included in the article's Creative Commons licence and your intended use is not permitted by statutory regulation or exceeds the permitted use, you will need to obtain permission directly from the copyright holder. To view a copy of this licence, visit http://creativecommons.org/licenses/by-nc-nd/4.0/.

© The Author(s) 2025